Int. J. Solids Structures, 1975, Vol. 11, pp. 679–691. Pergamon Press. Printed in Great Britain

STRESS WAVE PROPAGATION IN PLATES SUBJECTED TO A TRANSIENT LINE SOURCE

M. SHMUELY

Technion–Israel Institute of Technology, Department of Mechanics, Haifa, Israel

(*Received* 7 *July* 1974; *revised* 11 *September* 1974)

Abstract—A method of treating the response of plates to a transient load, which was recently proposed, is here elaborated for the particular case of a plate subjected to a transient line source. Expressions presenting the various stresses as functions of time and position are derived. A numerical scheme, by which these stresses are calculated, is described. Some results concerning the behavior of stresses in the course of time are illustrated and discussed.

INTRODUCTION

In[1] a general method is proposed for evaluating the stresses in an infinite plate subjected to a transient source. Let the infinite plate of thickness d based on a coordinate system (x, y, z), (see Fig. 1), be subjected to a line source

$$P = -F(t)Q\delta(x) \tag{1}$$

along the y axis. In equation (1) δ stands for Dirac delta function; $F(t)$ expresses the time dependence of the loading, restricted to obtain zero values for $t \leqslant 0$ and to yield piece-wise continuous derivatives with $F'(0) = 0$, but otherwise arbitrary. It is shown in[1] that if a two dimensional plain strain elastic problem is considered, the resulting Laplace transform of the two normal stresses σ_{zz} and σ_{xx}, and the shear stress σ_{xz}, can be expressed in the form

$$\bar{\boldsymbol{\sigma}}(x, z, s) = \begin{bmatrix} \bar{\sigma}_{zz}(x,z,s) \\ \bar{\sigma}_{xz}(x, z, s) \\ \bar{\sigma}_{xx}(x, z, s) \end{bmatrix} = s \sum_{n=0}^{\infty} \int_{-\infty}^{\infty} e^{ikzx}\, \mathbf{W}\mathbf{B}^n \mathbf{A}_0\, dk. \tag{2}$$

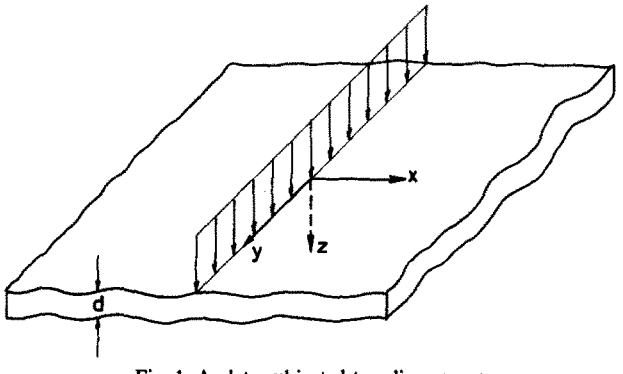

Fig. 1. A plate subjected to a line source.

In equation (2), s is the Laplace transform parameter; the infinite integrals are a consequence of applying Fourier transform to $\delta(x)$ with $\gamma = ks$ as the wave number; $\mathbf{W}$ is a (3×2) matrix of the form

$$\mathbf{W}=\begin{bmatrix} h & -g \\ -f & -h \\ r & g \end{bmatrix}\begin{bmatrix} e^{-s\nu z} & 0 \\ 0 & e^{-s\nu' z} \end{bmatrix}+\frac{q}{p}\begin{bmatrix} -h & -g \\ -f & h \\ -r & g \end{bmatrix}\begin{bmatrix} e^{-s\nu(2d-z)} & 0 \\ 0 & e^{-s\nu'(2d-z)} \end{bmatrix}$$

$$+\frac{1}{p}\begin{bmatrix} -(p-q)h & (p+q)g \\ (p+q)f & (p-q)h \\ (p-q)h & 2ghr \end{bmatrix}\begin{bmatrix} e^{-s[\nu d+\nu'(d-z)]} & 0 \\ 0 & e^{-s[\nu(d-z)+\nu' d]} \end{bmatrix}; \tag{3}$$

$\mathbf{B}$ is a (2×2) matrix of the form

$$\mathbf{B}=\frac{q}{p^2}\begin{bmatrix} q & 2gh \\ -2fh & q \end{bmatrix}\begin{bmatrix} e^{-s\nu 2d} & 0 \\ 0 & e^{-s\nu' 2d} \end{bmatrix}+\frac{1}{p^2}\begin{bmatrix} p^2-q^2 & -2ghq \\ 2fhq & p^2-q^2 \end{bmatrix}e^{-s[\nu d+\nu' d]}; \tag{4}$$

and

$$\mathbf{A}_0=\frac{Q}{2\pi p}\bar{F}(s)\begin{bmatrix} -h \\ f \end{bmatrix}. \tag{5}$$

In equations (3–5)

$$\nu=\sqrt{\left(\frac{1}{c_1^2}+k^2\right)};\quad \nu'=\sqrt{\left(\frac{1}{c_2^2}+k^2\right)};\quad f=2i\nu k;\quad g=2i\nu' k;$$
$$h=\nu'^2+k^2;\quad r=-h+2(\nu'^2-\nu^2);\quad p=h^2+fg;\quad q=h^2-fg. \tag{6}$$

In ν and ν' $c_1=[(\lambda+2\mu)/\rho]^{1/2}$ and $c_2=[\mu/\rho]^{1/2}$ represent the dilatational and distortional wave velocities respectively, where λ and μ are Lamé constants and ρ is the material density.

In equations (2) and (5) and hereafter, a bar over any given variable denotes its Laplace transform. In equation (2) and hereafter, an integration over a column matrix means the separate integration of each of its components.

The way the stresses are expressed in (2), involving summation over infinite series, is not the only one possible. Other expressions do exist, the form of which depends on the transformations employed and on the method by which the boundary conditions are introduced. In fact, as was proved in[1], series (2) converges to the compact form

$$\bar{\boldsymbol{\sigma}}(x,z,s)=s\int_{-\infty}^{\infty} e^{iksx}\,\mathbf{WCA}_0\,dk. \tag{7}$$

The last expression may be also derived by directly solving the plate problem applying a Laplace transform on the time variable and a Fourier transform on the spatial variable. In (7)

$$\mathbf{C}=\frac{p^2}{q^2(e^{-\nu sd}-e^{-\nu' sd})^2-p^2(1-e^{-s(\nu d+\nu' d)})}\{e^{-s(2d\nu+2d\nu')}\mathbf{B}^{-1}-\mathbf{I}\} \tag{8}$$

with $\mathbf{I}$ standing for the unit matrix.

The inverse transform of an expression like (7) is not straightforward. Using residue calculus and for a loading time variation of $F(t) = \delta(t)$, a modal form of solution [2] was proposed, which consists of an infinite sum of integrals, each of which represents a mode of propagation. Each mode is related to the roots of Rayleigh–Lamb frequency equation. (The last mentioned frequency equation is closely related to the denominator in (8)).

A different approach to the inverse transform of expressions like (7) was taken by Mencher [3], Broberg [4], Davids [5], and Rosenfeld and Miklowitz [6]. Starting from the double transforms, the denominator in the integrand (see equation 8) was expanded into a series of terms to yield expressions like (2), where exponents containing s appear only in the nominator of each term. In [1], however, instead of starting from (7), expression (2) is derived by superposing the contributions of the successive reflections at the plate surfaces. These contributions are added together while still in their transformed form. An analysis of a case similar to that treated here is found in [6], with the main concern there being the wave front behavior. The present work, however, is mainly concerned with the analysis of the dynamic stress configuration.

The advantage of employing an expression like (2), as demonstrated in [3–6] and hereafter, is two-fold. Firstly, each of the series terms in (2) is in a form susceptible to a solution technique, due to Cagniard, which enables the acomplishment of both the inverse Laplace transform and the inverse Fourier transform without actually performing the complicated double integration. Secondly, for any time of interest, only a well-defined finite number of terms are participating in the evaluation of stresses. Moreover, as already mentioned in defining $F(t)$ (see equation 1), $F(t)$ is such that a variety of practical situations are readily tackled.

In the following sections, the procedure of deriving the stress distribution in elastic plates will be described via considering numerical examples. Results concerning the stress state development is presented and discussed.

THE METHOD

Expanding the nth term in expression (2) yields

$$\bar{\sigma}_n(x, z, s) = \frac{Q}{2\pi} s\bar{F}(s) \sum_{j=1}^{2} \sum_{m=0}^{2n} \int_{-\infty}^{\infty} \mathbf{G}_\alpha e^{-s\{\nu[(2n-m)d+(2-j)z]+\nu'[md+(j-1)z]-ikx\}} dk$$

$$+ \frac{Q}{2\pi} s\bar{F}(s) \sum_{j=1}^{2} \sum_{m=0}^{2n+1} \int_{-\infty}^{\infty} \mathbf{G}_\beta e^{-s\{\nu[2n-m+1)d+(2-j)(d-z)]+\nu'[md+(j-1)(d-z)]-ikx\}} dk \tag{9}$$

where $\mathbf{G}_l$ are column matrices of order 3, each of which is a function of the parameters defined in (6), so that each $\mathbf{G}_l$ depends on the single argument k. The running indices α and β are equal to $(4n^2+2n+2m+j)$ and $(4n^2+6n+2m+j+2)$ respectively, which is in conformity with a total of $8n+6$ terms, corresponding to any given n.

Following a method originally due to Cagniard, the integrals in (9) are evaluated by considering k as a complex variable and by employing contour integration, with a contour so chosen that by an additional change of variable from k to τ we obtain [1]

$$\int_{-\infty}^{\infty} \mathbf{G}_l(k) e^{-s\tau} dk = \int_{\tau_l}^{\infty} 2 \,\text{Real}\left\{\frac{1}{(d\tau/dk)|_{k=k^+}} \mathbf{G}_l(k^+(\tau))\right\} e^{-s\tau} d\tau. \tag{10}$$

Note that τ, which is real and positive, comprises the exponent of the integrand in (9), excluding the factor $-s$, giving

$$\tau = \nu[(2n-m)d + (2-j)z] + \nu'[md + (j-1)z] - ikx \tag{11}$$

for terms appearing in the first line of (9); and

$$\tau = \nu[(2n-m+1)d + (2-j)(d-z)] + \nu'[md + (j-1)(d-z)] - ikx \tag{12}$$

for terms appearing in the second line of (9).

For any given real τ, equations (11) or (12) yield two roots of k which lie symmetrically with respect to the imaginary axis. k^+ in (10) denotes that root of (11) or (12) with its real value being positive or zero. Expressing k^+ explicitly in terms of τ is only possible when either the coefficient of ν is zero or that of ν' is zero. In all other cases, a special iterative procedure is needed to evaluate k^+.

τ_l in (10) is the τ corresponding to a pure imaginary $k_0{}^+$ which satisfies

$$\left.\frac{d\tau}{dk^+}\right|_{k=k_0{}^+} = 0 \tag{13}$$

provided $k_0{}^+ \leqslant i/c_1$. If $k_0{}^+ > i/c_1$, a situation which scarcely happens, τ_l should be replaced by $\tau_l{}^* = \tau(i/c_1)$. $\tau_l{}^*$ is always smaller than τ_l.

The integral on the right-hand side of (10) is easily seen to be the Laplace transform of

$$2\,\text{Real}\left[\frac{1}{(d\tau/dk)|_{k=k^+}} G_l(k^+(\tau))\right] H(\tau - \tau_l) \tag{14}$$

with $H(\tau)$ standing for the heaviside step function.

It follows that the inverse Laplace transform of each of the integrals in (9) is simply expressed by (14). Since all the integrals in (9) are multiplied by $s\bar{F}(s)$ (which is the Laplace transform of $F'(t)$), employing the convolution theorem and recalling that (9) represents only the nth term of (2), we finally obtain

$$\sigma(x, z, t) = \frac{Q}{\pi} \sum_{l=1}^{\infty} \int_0^t F'(t-\tau) H(\tau - \tau_l)\,\text{Real}\left[\frac{1}{(d\tau/dk)} G_l(\tau)\right] d\tau. \tag{15}$$

It is the sum in (15) that will be evaluated here yielding the sought stresses. First we note that for any given time t, only those terms in (15) do count with their $\tau_l < t$. Hence, the first step towards the final solution is the detection of those few terms, relevant at any specific time, out of the infinite number of terms appearing in (15). Of great help to the distinction of these last-mentioned special terms is the physical interpretation which may be attributed to any of the terms involved in (9), and hence in (15).

It is shown in [1] that each term in (9) represents, at least formally, the contribution to the state of stress at the point (x, z) of a group of waves distinguished by its specific propagation pattern. The characteristics of each pattern are determined by the structure of the associated exponent, expressed by τ. It is found that the number of the d multiples in the coefficient of ν in τ equals the

number of times that each of the waves, belonging to the same group, crosses the plate as a dilatational (P) wave, on its way from the source to the point (x, z) (see Fig. 2). Similarly the number of the d multiples in the ν' coefficient equals the number of times that the wave crosses the plate as a distortional (S) wave. The appearance of z (or $(d-z)$) in either the ν coefficient of the ν' coefficient indicates that the wave in question terminates as a P wave or an S wave respectively.

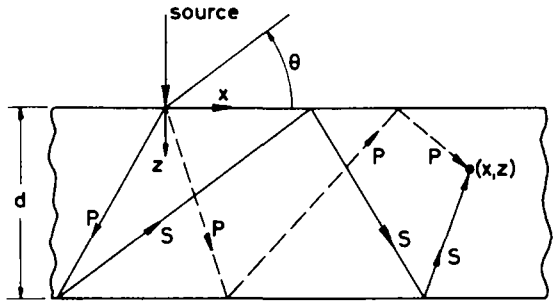

Fig. 2. Examples of wave paths corresponding to $n = 1$: ——— odd number of reflections corresponding to $\tau = \nu d + \nu'(2d + (d - z)) - ikx$; ------- even number of reflections corresponding to $\tau = \nu(2d + z) - ikx$.

From (9), or alternatively from (11) and (12), it follows that the wave groups represented by the nth term of (2), perform, in their course of propagation, a total number of either $2n$ (see expression 11) or $2n + 1$ (see expression 12) reflections at the free plate surfaces.

The significance of the above described physical interpretation lies in the fact that each τ_l is identical with the shortest time required from a wave, belonging to a group considered, to trace its way from the source to the point (x, z). The problem of deriving τ_l is thus reduced to finding a wave path, compatible with the pattern distinguishing the wave group considered, which yields the shortest time of travel. Given that the number of reflections is u we obtain for u even

$$\tau_l = \sqrt{[(ud + z)^2 + x^2]}/c_1 \tag{16}$$

if the wave pattern consists of P waves only;

$$\tau_l = \sqrt{[(ud + z)^2 + x^2]}/c_2 \tag{17}$$

if the wave pattern consists of S waves only; and

$$\tau_l = \frac{(u-m)d + (2-j)z}{c_1 \cos e_1} + \frac{md + (j-1)z}{c_2 \cos e_2} \tag{18}$$

for the case of mixed S and P waves. In (18), e_1 and e_2 satisfy Snell's law relation $(\sin e_1/c_1) = (\sin e_2/c_2)$ as well as the geometric condition $x = [(u-m)d + (2-j)z] \tan e_1 + [md + (j-1)z] \tan e_2$.

Similar equations are valid for u odd, but since in this case the waves approach the point (x, z) from the bottom of the plate, z in (16–18) should be replaced by $(d - z)$.

Comparing (16), (17) and (18), it is found that for any given number of reflections, u, τ_l as given in (16) is the shortest one. This τ_l, however, increases with u. Recalling that the number of reflections u increases with n ($u = 2n$ or $u = 2n + 1$), we conclude that for any given time of

interest t_f, there exists a number N such that all τ_l's associated with terms satisfying $n \geq N$ are equal or exceed t_f. From (16) we obtain that N equals to the least n which satisfies

$$t_f \leq [(2nd + z)^2 + x^2]^{1/2}/c_1 \tag{19}$$

Thus, given t_f and hence N, the series (2) can be truncated at $n = N$. When the remainder of (2) is further expanded into the elementary terms as described in (9), an additional truncation takes place involving those $\mathbf{G}_l$ with their τ_l still greater than t_f. The truncation process will be illustrated later by an example.

The next step towards the final solution is the derivation of all relevant $\mathbf{G}_l$'s. This implies the multiplication of the matrices appearing in (2) and defined in (3), (4), (5) and (6). The details of this step are here omitted but the results are summed up in Table 1. In Table 1 and hereafter, the dimensionless time $(c_1 t/d)$ is used so that a unit of time is the time required by a P wave to cross the plate. Poisson's ratio is taken as 0·25 so that $c_1^2/c_2^2 = 3$, z and x are given as multiples of d with $d = 1$ constituting the unit of length. All results are restricted to the contribution of the first three $(n = 0, 1, 2)$ terms in (2). This means that results are valid only up to the time at which the first wave, that has performed six successive reflections, reaches (x, z). From (16) or (19) (with $N = 3$) we obtain

$$\frac{c_1}{d} t_f = \frac{c_1}{d} \sqrt{[(6d + z)^2 + x^2]}/c_1 = \sqrt{\left[\left(6 + \frac{z}{d}\right)^2 + \left(\frac{x}{d}\right)^2\right]}. \tag{20}$$

In Table 1

$$\mathbf{E}_1 = \begin{bmatrix} h \\ -f \\ r \end{bmatrix}; \quad \mathbf{E}_2 = \begin{bmatrix} -g \\ -h \\ g \end{bmatrix}; \quad \mathbf{E}_3 = \begin{bmatrix} h \\ f \\ r \end{bmatrix}; \quad \mathbf{E}_4 = \begin{bmatrix} -g \\ h \\ g \end{bmatrix}. \tag{21}$$

The numerical results given in the seventh column correspond to a case where $x/d = 1{\cdot}2$ and $z/d = 0{\cdot}6$. In this case, equation (20) yields $(c_1/d)t_f = 6{\cdot}7082$. The last value implies (see the last two columns) that no more than 30 out of the 42 wave groups listed in Table 1 are to be summed up when (15) is evaluated. For times of interest t shorter than t_f even fewer terms are needed. In the just-mentioned example, it happens twice that (13) yields $k^+ = k_0^+ > i/c_1$. In both cases (see rows 2 and 6) we find that $\tau_l^* = \tau(i/c_1)$ is indeed smaller than $\tau_l(k_0^+)$.

THE NUMERICAL SCHEME

Although Table 1 includes all the information needed to evaluate stresses from expression (15), the job of calculating these stresses is still far from straight-forward. Some remarks concerning the numerical scheme used and indicating the techniques employed may be helpful.

First we decide upon the form of $F(t)$, the time variation of the load. $F(t)$ is chosen to consist of two third-order parabola segments, both starting and terminating with zero slopes (see Fig. 3). The rise time interval and decay time interval are Δ_1 and Δ_2 respectively, so that

$$F(t) = \begin{cases} -2t^3/\Delta_1^3 + 3t^2/\Delta_1^2 & 0 \leq t \leq \Delta_1 \\ 1 + 2(t - \Delta_1)^3/\Delta_2^3 - 3(t - \Delta_1)^2/\Delta_2^2 & \Delta_1 \leq t \leq \Delta_1 + \Delta_2 \\ 0 & 0 \geq t \geq \Delta_1 + \Delta_2 \end{cases}. \tag{22}$$

By changing the values of Δ_1 and Δ_2 we can approximate various practical loading conditions.

Table 1.

1 Serial no. (l)	2 Term no. (n)	3 No. of reflections u	4 Wave pattern	5 G_l	6 τ	7 $(c_1/d)\tau_l$	8 Truncation no	9 Truncation yes
1		0	P	$[-h/p]\mathbf{E}_1$	$\nu(z)-ikx$	1·3416	√	
2			S	$[f/p]\mathbf{E}_2$	$\nu'(z)-ikx$	2·3248 2·0485†	√	
3	0		PP	$(qh/p^2)\mathbf{E}_3$	$\nu[d+(d-z)]-ikx$	1·8439	√	
4		1	PS	$[-f(p+q)/p^2]\mathbf{E}_4$	$\nu[d]+\nu'[d-z]-ikx$	2·1882	√	
5			SP	$[(p-q)h/p^2]\mathbf{E}_3$	$\nu[d-z]+\nu'[d]-ikx$	2·7399	√	
6			SS	$[qf/p^2]\mathbf{E}_4$	$\nu'[d+(d-z)]-ikx$	3·1937 3·1799†	√	
7			PPP	$[-hq^2/p^3]\mathbf{E}_1$	$\nu[2d+z]-ikx$	2·8636	√	
8			PPS	$[fq(p+q)/p^3]\mathbf{E}_2$	$\nu[2d]+\nu'[z]-ikx$	3·3297	√	
9		2	PSP	$[h(2q^2-qp-p^2)/p^3]\mathbf{E}_1$	$\nu[d+z]+\nu'[d]-ikx$	3·6441	√	
10			PSS	$[f(p^2-qp-2q^2)/p^3]\mathbf{E}_2$	$\nu[d]+\nu'[d+z]-ikx$	4·1230	√	
11			SSR	$[hq(p-q)/p^3]\mathbf{E}_1$	$\nu[z]+\nu'[2d]-ikx$	4·4496	√	
12			SSS	$[fq^2/p^3]\mathbf{E}_2$	$\nu'[2d+z]-ikx$	4·9598	√	
13	1		PPPP	$[hq^3/p^4]\mathbf{E}_3$	$\nu[3d+(d-z)]-ikx$	3·6056	√	
14			PPPS	$[-fq^2(p+q)/p^4]\mathbf{E}_4$	$\nu[3d]+\nu'[(d-z)]-ikx$	3·9088	√	
15			PPSP	$[hq(-3q^2+pq+2p^2)/p^4]\mathbf{E}_3$	$\nu[2d+(d-z)]+\nu'[d]-ikx$	4·3658	√	
16		3	PPSS	$[f(p+q)(3q^2-pq-p^2)/p^4]\mathbf{E}_4$	$\nu[2d]+\nu'[d+(d-z)]-ikx$	4·6724	√	
17			PSSP	$[h(p-q)(p^2-pq-3q^2)/p^4]\mathbf{E}_3$	$\nu[d+(d-z)]+\nu'[2d]-ikx$	5·1357	√	
18			PSSS	$[fq(2p^2-pq-3q^2)/p^4]\mathbf{E}_4$	$\nu[d]+\nu'[2d+(d-z)]-ikx$	5·4476	√	
19			SSSP	$[hq^2(p-q)/p^4]\mathbf{E}_3$	$\nu[(d-z)]+\nu'[3d]-ikx$	5·9221	√	
20			SSSS	$[fq^3/p^4]\mathbf{E}_4$	$\nu'[3d+(d-z)]-ikx$	6·2450	√	
21			PPPPP	$[-hq^4/p^5]\mathbf{E}_1$	$\nu[4d+z]-ikx$	4·7539	√	
22			PPPPS	$[f(q^4+pq^3)/p^5]\mathbf{E}_2$	$\nu[4d]+\nu'[z]-ikx$	5·2020	√	
23			PPPSP	$[h(4q^4-pq^3-3q^2p^2)/p^5]\mathbf{E}_1$	$\nu[3d+z]+\nu'[d]-ikx$	5·5013	√	
24			PPPSS	$[-f(4q^4+3pq^3-3q^2p^2-2qp^3)/p^5]\mathbf{E}_2$	$\nu[3d]+\nu'[d+z]-ikx$	5·9513	√	
25		4	PPSSP	$[h(-6q^4+3pq^3+6q^2p^2-2qp^3-p^4)/p^5]\mathbf{E}_1$	$\nu[2d+z]+\nu'[2d]-ikx$	6·2521	√	
26			PPSSS	$[f(6q^4+3pq^3-6q^2p^2-2qp^3+p^4)/p^5]\mathbf{E}_2$	$\nu[2d]+\nu'[2d+z]-ikx$	6·7048	√	
27			PSSSP	$[h(4q^4-3pq^3-3q^2p^2+2qp^3)/p^5]\mathbf{E}_1$	$\nu[d+z)+\nu'[3d]-ikx$	7·0078		√
28			PSSSS	$[f(-4q^4-pq^3+3q^2p^2)/p^5]\mathbf{E}_2$	$\nu[d]+\nu'[3d+z]-ikx$	7·4645		√
29			SSSSP	$[h(-q^4+pq^3)/p^5]\mathbf{E}_1$	$\nu[z]+\nu'[4d]-ikx$	7·7708		√
30			SSSSS	$[fq^4/p^5]\mathbf{E}_2$	$\nu'[4d+z]-ikx$	8·2341		√
31	2		PPPPPP	$[hq^5/p^6]\mathbf{E}_3$	$\nu[5d+(d-z)]-ikx$	5·5317	√	
32			PPPPPS	$[-fq^4(p+q)/p^6]\mathbf{E}_4$	$\nu[5d]+\nu'[d-z]-ikx$	5·8287	√	
33			PPPPSP	$[h(-5q^5+pq^4+4p^2q^3)/p^6]\mathbf{E}_3$	$\nu[4d+(d-z)]+\nu'[d]-ikx$	6·2748	√	
34			PPPPSS	$[f(5q^5+4pq^4-4p^2q^3-3q^2p^3)/p^6]\mathbf{E}_4$	$\nu[4d]+\nu'[d+(d-z)]-ikx$	6·5726	√	
35			PPPSSP	$[h(10q^5-4pq^4-12p^2q^3+3q^2p^3+3qp^4)/p^6]\mathbf{E}_3$	$\nu[3d+(d-z)]+\nu'[2d]-ikx$	7·0200		√
36		5	PPPSSS	$[f(-10q^5-6pq^4+12p^2q^3+6q^2p^3-3qp^4-p^5)/p^6]\mathbf{E}_4$	$\nu[3d]+\nu'[2d+(d-z)]-ikx$	7·3187		√
37			PPSSSP	$[h(-10q^5+6pq^4+12p^2q^3-6q^2p^3-3qp^4+p^5)/p^6]\mathbf{E}_3$	$\nu[2d+(d-z)]+\nu'[3d]-ikx$	7·7678		√
38			PPSSSS	$[f(10q^5+4pq^4-12p^2q^3-3q^2p^3+3qp^4)/p^6]\mathbf{E}_4$	$\nu[2d]+\nu'[3d+(d-z)]-ikx$	8·0679		√
39			PSSSSP	$[h(5q^5-4pq^4-4p^2q^3+3q^2p^3)/p^6]\mathbf{E}_3$	$\nu[d+(d-z)]+\nu'[4d]-ikx$	8·5194		√
40			PSSSSS	$[f(-5q^5-pq^4+4p^2q^3)/p^6]\mathbf{E}_4$	$\nu[d]+\nu'[4d+(d-z)]-ikx$	8·8241		√
41			SSSSSP	$[hq^4(p-q)/p^6]\mathbf{E}_3$	$\nu[d-z]+\nu'[5d]-ikx$	9·2763		√
42			SSSSSS	$[fq^5/p^6]\mathbf{E}_4$	$\nu'[5d+(d-z)]-ikx$	9·5812		√

†Equation (13) yields $k_0^* > i/c_1$; the right-hand number corresponds to $\tau_l^* = \tau(i/c_1)$.

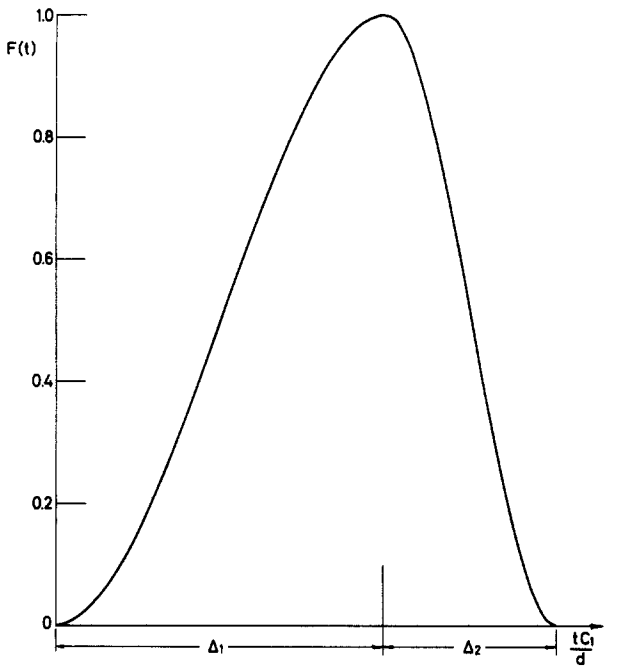

Fig. 3. Time dependence of the loading.

Next we decide upon a series of positions inside the plate, where the time variation of the stresses are to be determined. For each such position the following steps are taken.

From equation (20) the time t_f is derived. The time interval $(0, t_f)$ is then divided into small segments Δt yielding a set of discrete points t. At each t the stresses are determined by (15), summing up the contributions of all the wave groups listed in Table 1. We consider each wave group at a time. Turning to the corresponding row in Table 1, we first find τ_l. For this purpose equations (16–18), or their counterparts (with z replaced by $(d - z)$), are employed. Note that the derivation of (18) involves a special iteration process. Recall that the just-mentioned τ_l's correspond to $k^+ = k_0^+$ which yield $d\tau/dk = 0$, and that in case $k_0^+ > i/c_1$ we replace τ_l, in the argument of the Heaviside function, by $\tau_l^* = \tau(i/c_1)$.

If τ_l (or alternatively τ_l^*) exceeds t, the corresponding row is skipped, since no contribution is expected, at the point (x, z) at time t, from waves represented by that row. For τ_l (or τ_l^*) smaller than t, the lth integral of (15) is performed numerically by the trapezoidal rule. To this end the integrand in (15) is evaluated at points τ on the interval (τ_l, t) (or (τ_l^*, t)), which are equidistantly separated by the distance $\Delta\tau$. The $\Delta\tau$ is chosen to be numerically equal to the time step Δt, used in determining t. Moreover, the points of division τ are so adjusted as to coincide numerically with the points of division t. The last adjustment is introduced in order to save the repeated computation of terms like Real $\{(1/(d\tau/dk))\mathbf{G}_l\}$ or $F'(t - \tau)$, the values of which are needed again when stresses are derived at more advanced times t. In the course of integration a difficulty arises at $\tau = \tau_l$ since the integrand has a singularity there ($d\tau/dk = 0$). The integration, however, is still possible as the residue at that point is zero. The last facts imply the evaluation of the integrand at additional points τ which are obtained by further dividing the $\Delta\tau$, lying next to τ_l, into smaller segments $\Delta^\dagger\tau$. The last-mentioned integrand values do participate in the integration process. They are also used in extrapolating a value which is to be substituted for the integrand value at τ_l.

For each τ, the integrand is derived by the following method. First we find the corresponding k^+. This is accomplished by either expressing, if possible, k in terms of τ, or by an appropriate iteration process. With the k^+ obtained substituted in G_l and $d\tau/dk$, the value of Real $\{(1/(d\tau/dk))G_l\}$ is derived. The last-mentioned value is then multiplied by $F'(t-\tau)$.

The actual numerical scheme, although based on the steps outlined above, was not executed in the above described order. Some changes were introduced with the benefit of shorter computing times and a clearer representation of results. Values of variables which are repeatedly used in various steps of the integration process, are calculated and stored in appropriate arrays. Thus, before referring to any particular point (x, z), the values of $F'(t)$, given at equidistant points $t_i = i\,\Delta t$ $(i = 0, 1, 2, \ldots (\Delta_1 + \Delta_2)/\Delta t)$, are tabulated in one array DF_i. Next, for each point (x, z) and before referring to any particular time of interest t, we scan the 42 wave groups listed in Table 1, gathering all the information needed for the final integrations. The component values of 2 Real $\{G_l/(d\tau/dk)\}$, given at equidistant points $\tau_m = m\Delta\tau (m = j_l, j_l + 1, \ldots, j_f;\ j_l = [\tau_l/\Delta\tau]\dagger + 1$ and $j_f = [t_f/\Delta\tau])$, are tabulated in a three dimensional array G_{lmn}. The subscripts l, m and n correspond respectively to the wave group, the time step, and the stress component considered. A separate three dimensional array GS_{lqn} is constructed to account for values of 2 Real $\{G_l/d\tau/dk)\}$, given at the equidistant points $\tau_q = \tau_l + q\Delta\dagger\tau$ $(q = 1, 2, \ldots, q_l;\ q_l = (j_l\Delta\tau - \tau_l)/\Delta\dagger\tau)$ which lie near the singularities $\tau = \tau_l$. Other arrays give the values of τ_l, j_l, q_l and $\Delta\dagger\tau$. The entries of another very helpful array W_p $(p = 1, 2, \ldots 42)$ consist of all the serial numbers designating the various wave groups. W_p is so arranged that τ_l's corresponding to wave groups listed in sequential elements of W_p are in an ascending order.

With all the aforementioned information in hand we proceed towards the evaluation of (15) at times $t = r\Delta t$ $(r = j_1, j_1 + 1, \ldots j_f)$. Given t, we first determine the lower limit τ_0 of the time interval on which the integrations will be performed. If $t > (\Delta_1 + \Delta_2)$, $\tau_0 = t - (\Delta_1 + \Delta_2)$ since, for $\tau < t - (\Delta_1 + \Delta_2)$, $F'(t - \tau) = 0$. If $t < (\Delta_1 + \Delta_2)$, $\tau_0 = (j_1 - 1)\Delta\tau$ since the arrival time of the first group of waves is τ_1, and $j_1 = [\tau_1/\Delta\tau] + 1$. We now sum up the contributions of the various wave groups, which are selected in the order that they appear in W_p. When considering the lth wave group, which is listed in, say, the pth element of W_p, we are first concerned with the corresponding τ_l value as related to either t or τ_0. If $\tau_l > t$ the evaluation of stresses at time t is completed, the results obtained so far by summing up the $p - 1$ relevant terms of (15) are recorded, and we turn to the next time step $t = (r + 1)\Delta t$. If $\tau_l < \tau_0$ the integration of the lth term of (15) is performed over the interval $\tau_0 \leqslant \tau \leqslant t$, using the values of $F'(t - \tau)$ and 2 Real $\{G_l/(d\tau/dk)\}$, which have been already calculated and are recorded in DF_{r-m} and G_{lmn} respectively. If $\tau_0 < \tau_l < t$ the integration is performed over the interval $\tau_l < \tau \leqslant t$ in two steps. On the interval $\tau_l < \tau < j_l\Delta\tau$ we refer to GS_{lqn} instead of to G_{lmn}, and $F'(t - \tau_q)$ is calculated whenever needed. On the rest of the interval we employ again the appropriate values from DF_i and G_{lmn}.

SOME NUMERICAL RESULTS

The results which are described in the following correspond to a loading time variation $F(t)$ with a dimensionless time rise $\Delta_1 = 4{\cdot}35$ and time decay $\Delta_2 = 2{\cdot}25$. The last values are in conformity with measurements taken for line explosives. To obtain the dimensionless Δ_1 and Δ_2 a plate made of perspex of 6 mm thickness was assumed. For thicker plates or other materials Δ_1 and Δ_2 should obviously be changed but the ratio Δ_1/Δ_2 must be kept.

†The brackets indicate that the largest integer whose magnitude does not exceed the magnitude of the variable inside the brackets is used.

Stresses were evaluated in region $0{\cdot}2 \leqslant x/d \leqslant 2{\cdot}0$, $0{\cdot}1 \leqslant z/d \leqslant 1{\cdot}0$ with increments of $x/d = 0{\cdot}2$ in the x direction and $z/d = 0{\cdot}1$ in the z direction. In addition to the stresses σ_{xx}, σ_{zz} and σ_{xz}, the corresponding principal stresses σ_1 and σ_2 were also calculated. By σ_1 we denote that principal stress which forms an angle $0° \leqslant \theta \leqslant 90°$ with the x axis, with θ taken as positive in the counter-clockwise direction (see Fig. 2). All calculations were performed on an IBM 370/165 computer. About 3 sec of computation time is needed for each spatial point.

In Fig. 4 the development of the five stresses at the point $(x/d = 1{\cdot}0, z/d = 0{\cdot}5)$ is illustrated. The last mentioned point lies in the middle of the region examined. The arrival times of the various wave groups discussed in the previous sections are also depicted. At the point in question, the period covered by our calculations starts at $(c_1 t/d) = 1{\cdot}1180$, which corresponds to the arrival time of the first group of waves (the P group), and ends at $(c_1 t/d) = 6{\cdot}5765$ as obtained from equation (20). Note that at the just-mentioned period of time, only 28 groups of waves contribute to the state of stresses, since the remaining groups arrive, at the point in question, later.

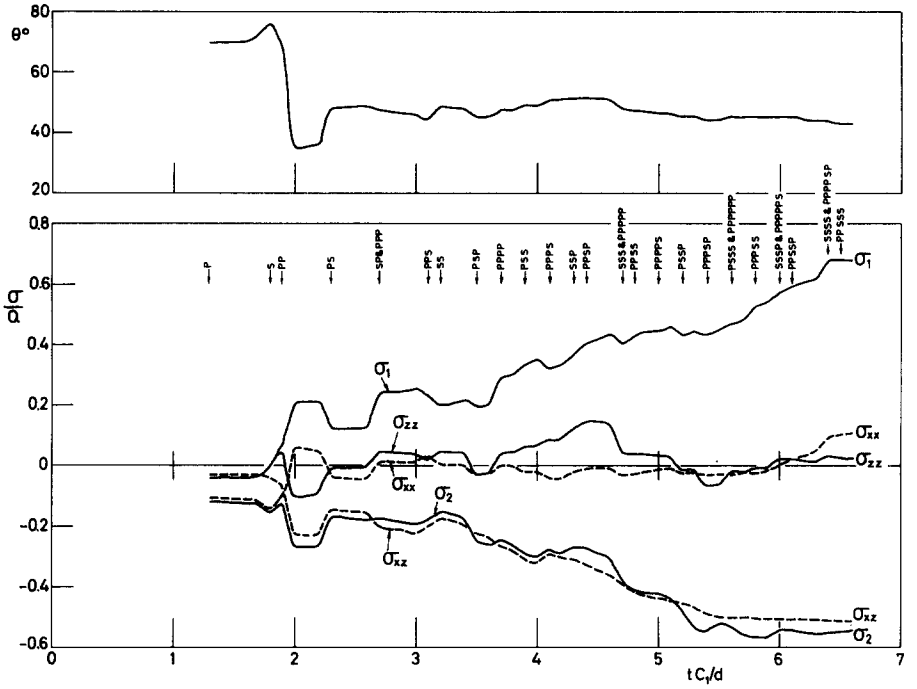

Fig. 4. Normal, shear and principal stresses and direction of principal stresses at the point $(x = d, z = 0{\cdot}5d)$.

Due to the dispersive nature of stress wave propagation in plates, it is expected that the development of the various stresses, as related to different spatial points, will show no common features of behaviour. This is indeed the case with the developing pattern of σ_{xx}, σ_{zz} or σ_{xz}. An interesting exception is the behaviour of the principal stresses, provided they are grouped in the manner described above, namely, σ_1 is always the principal stress normal to planes which intersect the first quadrant, while σ_2 is perpendicular to it. As demonstrated in Fig. 4, σ_1 rises, in the course of time, to relatively high positive (tensile) levels, while its direction, which is also depicted in the figure, forms, with the x axis, by the end of the time covered in the figure, an angle

of about 40°. The rise of σ_1 to positive values is encountered in almost all the points examined excluding points near or at the bottom of the plate ($z = d$), and few additional points in the proximity of the source. The associated second principal stress (σ_2), however, builds up in most of the points (excluding some points near the source) to either negative (compressive) values or, compared with σ_1, small positive values. By comparing the σ_1 stress levels across the plate for a given fixed x, one finds (see Fig. 5) that higher tensile stress levels are encountered at the upper parts of the plate ($z \leq 0{\cdot}5d$), provided $x \geq d$. At cross sections which are closer to the source, there is no significant difference between the σ_1 stress levels at the upper and lower parts of the plate. (In Fig. 5, being mainly interested in the right-hand section of it, and since the left-hand section would be crowded together if all the informations were depicted, some of the curves are started at later times.) The occurrence of high tensile stresses, located and directed as they happen to be, explains quite satisfactorily the experimental observations mentioned in [1].

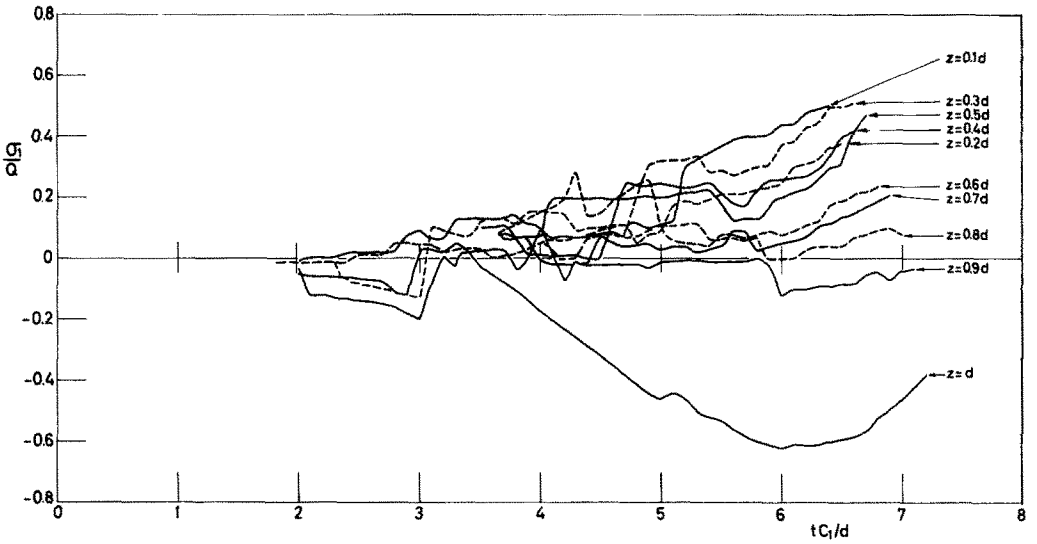

Fig. 5. Principal stresses across the plane $x = 1{\cdot}6d$.

Finally, we mention some results of an investigation which has been carried out, the purpose of which was to find out whether, under the above described circumstances, any of the plate free vibrational modes is dominant. We expect such modes, if they exist, to appear only after a considerable time has elapsed and at points which lie sufficiently far from the source. To this end we refer to the amplitude spectra of the stresses involved. Relevant spectra are obtained by a Fourier analysis, with respect to wave numbers, of stresses evaluated at a given fixed time, located at points lying in the mid-plane ($z = 0{\cdot}5d$), along a given interval. Note that in the mid-plane the symmetric modes of propagation are readily distinguished from the antisymmetric (flexural) modes, by referring separately to the normal stresses and shear stresses respectively.

As long as the scheme described in this paper is employed, the x interval, on which the analysis can be conducted, is restricted, at a given time t, to $(c_1t)^2 - (6{\cdot}5d)^2 < x^2 < (c_1t)^2 - (0{\cdot}5d)^2$ (see equation 20). This means that for higher values of time, the x interval on which information is available, although shifting, as a whole, away from the source, is getting shorter. With shorter intervals, conclusions drawn from a direct Fourier analysis are doubtful and special techniques

are needed to obtain meaningful results [7]. The last mentioned techniques which were applied to intervals corresponding to relatively high values of time, confirmed the results reported hereafter.

For a dimensionless time of 6·5, with a corresponding interval of $1{\cdot}1d < x < 6{\cdot}1d$, significant peaks are detected in the σ_{xx} and σ_{zz} amplitude spectra (see Fig. 6). To obtain these spectra, stresses were evaluated at 250 points lying equidistantly on the aforementioned interval, and the subroutine RHARM, provided by IBM [8] was employed. The peak in the σ_{xx} spectrum corresponds to a wave number of $k_1 \simeq 4{\cdot}6/d$, while that in the σ_{zz} spectrum—to a wave number of $k_2 \simeq 3{\cdot}7/d$. Referring to available solutions of the Rayliegh–Lamb frequency equations [9] and in particular to the lowest branch of the symmetric modes, we find that k_1 corresponds to a

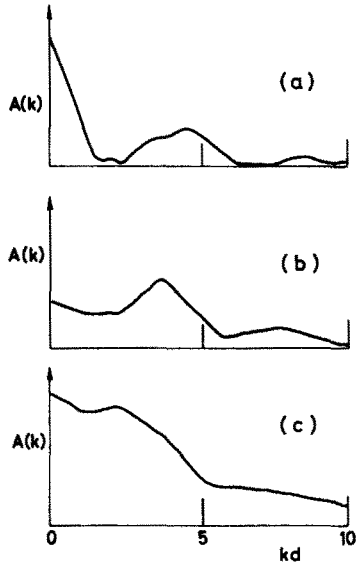

Fig. 6. Amplitude spectra of: (a) σ_{xx}; (b) σ_{zz}; (c) σ_{xz}.

frequency $\omega_1 \simeq 5{\cdot}3c_2/d$ which yields a period of $T_1 \simeq 1{\cdot}18c_1/c_2\, d/c_1 \simeq 2{\cdot}05d/c_1$. The last value is approximately the time required for dilatational waves to cross the plate thickness twice. This means that the frequency of the dominating mode is related to the oscillations of those dilatational waves which are travelling at $x = 0$, back and forth between the two plate surfaces. No similar correlation was found with k_2. But, if half of that wave number is considered, namely, $k = 1{\cdot}85/d$, we end with a period of $T_2 \simeq 2{\cdot}05d/c_2$, which may be related to the oscillations at $x = 0$, of distortional waves. Since the σ_{xz} spectrum (see Fig. 6), as obtained from the direct Fourier analysis, shows no distinctive peaks, the analysis was applied to the autocovariance function of the given data. The resulting σ_{xx} and σ_{zz} spectra yield again peaks at the same wave numbers as before. The resulting σ_{xz} spectrum although indicating the existence of a dominating flexural mode, the corresponding wave number $k_3 \simeq 1{\cdot}84/d$ shows no correlation to any of the frequencies mentioned above.

REFERENCES

1. M. Shmuely, Response of plates to transient sources. *J. Sound Vibr.* **32** (4), 491 (1974).
2. P. W. Randles and J. Miklowitz, Modal representation for the high-frequency response of elastic plates. *Int. J. Solids Struc.* **7**, 1031 (1971).
3. A. G. Mencher, Epicentral displacements caused by elastic waves in an infinite slab. *J. Appl. Phys.* **24**, 1240 (1953).

4. K. B. Broberg, A problem on stress waves in an infinite elastic plate. *Trans. Roy. Inst. Tech.* Stockholm, Rep. No. 139 (1959).
5. N. Davids, Transient analysis of stress-wave penetration in plates. *J. Appl. Mech.* **26**, 651 (1959).
6. R. L. Rosenfeld and J. Miklowitz, Wave fronts in elastic rods and plates. *Proc. 4th Nat. Cong. Appl. Mech.* 293 (1962).
7. G. M. Jenkins and D. G. Watts, *Spectral Analysis and its Application.* Holden-Day, San Francisco (1968).
8. I.B.M., System/360 Scientific Subroutine Package. Publication No. H-20-0205-03.
9. J. D. Achenbach, *Wave Propagation in Elastic Solids.* North-Holland, Amsterdam (1973).